Hypersonic phonon propagation in one-dimensional surface phononic crystal

B. Graczykowski,[1,a)] M. Sledzinska,[1] N. Kehagias,[1] F. Alzina,[1] J. S. Reparaz,[1] and C. M. Sotomayor Torres[1,2]
[1]*ICN2 - Institut Catala de Nanociencia i Nanotecnologia, Campus UAB, 08193 Bellaterra (Barcelona), Spain*
[2]*ICREA - Institucio Catalana de Recerca i Estudis Avançats, 08010 Barcelona, Spain*

(Received 4 December 2013; accepted 16 March 2014; published online 28 March 2014)

Hypersonic, thermally activated surface acoustic waves propagating in the surface of crystalline silicon patterned with periodic stripes were studied by Brillouin light scattering. Two characteristic directions (normal and parallel to the stripes) of surface acoustic waves propagation were examined exhibiting a distinctive propagation behavior. The measured phononic band structure exhibits diverse features, such as zone folding, band gap opening, and hybridization to local resonance for waves propagating normal to the stripes, and a variety of dispersive modes propagating along the stripes. Experimental results were supported by theoretical calculations performed using finite element method.
[http://dx.doi.org/10.1063/1.4870045]

Studies on the phonon engineering have been gaining importance in recent 20 yr. Previous research has shown that phonon dispersion relation can be significantly modified by means of phononic crystals (PnCs),[1–3] spatial confinement,[4–6] or external stress field.[7–10] Phononic crystals are in general materials with one- (1D), two-, or three-dimensional periodicity in their elastic properties. This spatial modulation with a proper choice of acoustic impedances and geometric features can lead to the appearance of forbidden frequencies (phononic band gaps) at which propagation of acoustic waves/phonons is not allowed. The origin of the phononic band gaps lies in two different mechanisms, Bragg reflections and local mechanical resonances.[2,11,12] Another approach to modify phonon dispersion relies on spatial confinement. The dynamic behavior at reduced characteristic dimensions has been found to be completely different than for bulk materials. It has been shown that spatial confinement modifies the acoustic waves in nanowires and ultra-thin membranes, which can affect their thermal and electronic properties.[5,6,13–17] Along with extensive research on PnCs, the studies on surface acoustic waves (SAWs) propagation in periodic structures were resumed. The first experimental and theoretical studies of Rayleigh surface waves (RSWs) propagation across single or periodic surface corrugations were started in the seventies.[18,19] It was proved that one-dimensional (1D) surface gratings introduce new zone boundaries and zone folding of the dispersion relations and also frequency band gaps.[20,21] However, the previous studies were focused on the analysis of structures with surface corrugations much shallow than the given SAW wavelength. Therefore, e.g., SAWs propagating parallel to the grooves were found to be practically undisturbed by the presence of the grating.[20]

In this paper, we consider 1D surface phononic crystal (SPnC) in the form of rectangular-like periodic grooves made on the (001) surface of crystalline silicon. Contrary to previous reports, we examine structures with grooves depth comparable to the SAW wavelength to confine part or the whole of the acoustic field within the rectangular stripes. The surface gratings were fabricated in a silicon wafer, which was coated with a 50 nm thick poly (methyl methacrylate) (PMMA) film. Grooves were defined along the [110] direction of Si in PMMA by electron beam lithography (Vistec EBPG5000 Plus) at 100 kV. The pattern was transferred to Si by dry etching in an inductively coupled plasma (ICP) reactive ion etcher (Alcatel Nextral NE 330) using SF_6, N_2, and O_2 gas mixtures with flows of 15, 10, and 10 sccm, respectively, and at the constant pressure of 5 mTorr. Measurements were performed on the samples with a surface grating of period $a = 300$ nm and crystallographic orientation as shown in Fig. 1(a). A cross-section of the unit cell used in finite element method (FEM) calculations is presented in Fig. 1(b). It is based on an image obtained by focused ion beam (Zeiss 1560XB Cross Beam) measurements. The real shape of stripes cross section is approximated by a rectangle with width $b = 60$ nm, height $h = 120$ nm, and two additional elements with a curvature radius of $r = 50$ nm. In order to get the exponential decay of the SAW amplitude with depth, we assumed free boundary conditions for the upper part of the unit cell and fixed boundary conditions for the bottom of the unit cell (see Fig. 1(b)). For FEM calculations, the structure must be finite but we need to approach to a semi-infinite like substrate. Therefore, the height of the remaining part of the unit cell (Si substrate) was made to be dependent on the SAW wavelength so that $H = 4\lambda_{SAW}$. The Bloch-Floquet periodic boundary conditions were applied for the boundaries normal to x_1 and x_2 axes (see Fig. 1(b)). The calculations were performed for the elastic constants of cubic silicon $C_{11} = 165.7$ GPa, $C_{12} = 63.9$ GPa, $C_{44} = 79.9$ GPa, and the mass density $\rho = 2331\,\mathrm{kg/m^3}$. From all the calculated undamped mechanical eigenmodes satisfying the above boundary conditions, only the ones which correspond to surface-like waves were selected by means of the parameter

[a)]Author to whom correspondence should be addressed. Electronic mail: bartlomiej.graczykowski@icn.cat.

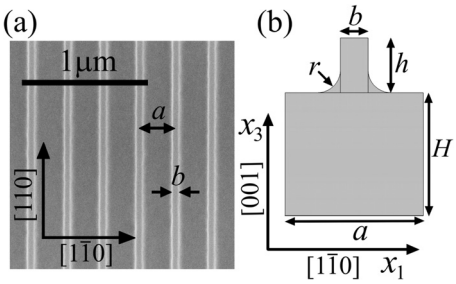

FIG. 1. (a) Scanning electron microscope image of the studied sample, (b) schematic presentation of the FEM unit cell cross section.

$$\xi = \left(1 - \frac{\int_V F x_3 dV}{H \int_V F dV}\right), \quad (1)$$

where F denotes elastic free energy density.[2,22] Measurements of the dispersion relations of SAWs propagating in 1D SPnC were performed by means of Brillouin light scattering (BLS). Brillouin spectroscopy, based on the high-resolution tandem type Fabry-Perot spectrometer (JRS Instruments), enables studies of thermally activated bulk and surface acoustic waves (phonons) in the hypersonic range. In the BLS measurements, we used *p–p* and *p–s* backscattering geometries with the incident light wavelength of $\lambda_0 = 532$ nm. Here, according to the common notation, *p* denotes light polarized parallel to the sagittal plane and *s* normal to it.[23,24] In this case, the magnitude of the scattering wavevector **q** is given by: $q = 4\pi \sin\theta/\lambda_0$, where θ is the incident and scattered light angle.[24] For periodic structures the scattering wave vector is defined by momentum conservation: $\mathbf{q} = \mathbf{k} + \mathbf{G}$, where **G** denotes the reciprocal lattice vector. For the waves propagating normal to the stripes the magnitude of **q** is given by $q = k + 2n\pi/a$, where n is an integer and a is the SPnC lattice constant. For SAWs propagating parallel to the stripes $G = 0$ and, therefore the wavevector **q** and the wavevector **k** of a surface wave are equal.

The BLS experiments were performed at room temperature for SAWs propagating in two mutually perpendicular directions: [110] and [1$\bar{1}$0] on the (001) plane of Si. Two particular BLS spectra obtained for SAWs at $q = 0.020456$ nm^{-1} propagating in the [110] direction (**q** parallel to the stripes) are shown in Fig. 2(a). In principle, measuring both in *p–p* and *p–s* configurations allows to distinguish the SAWs in terms of their total displacement. In Fig. 2(a), for the *p–s* geometry, a pair of symmetric peaks is visible. These peaks, labeled A, are related to the SAWs polarized normal to the sagittal plane. Their average position gives information about the Brillouin shift, which is the frequency of SAW for a given **q**. For the *p–p* geometry the observed doublets of peaks labeled B, C, and D can be identified as coming from the SAWs polarized parallel to the sagittal plane. The polarizations of all the observed waves were verified by means of FEM calculations shown in Fig. 2(b). Mode A is then associated to the 3D displacement field, which clearly indicates a mechanical wave polarized in the x_1 x_2 plane and confined mainly in the stripe. Moreover, if one considers x_2x_3 plane as

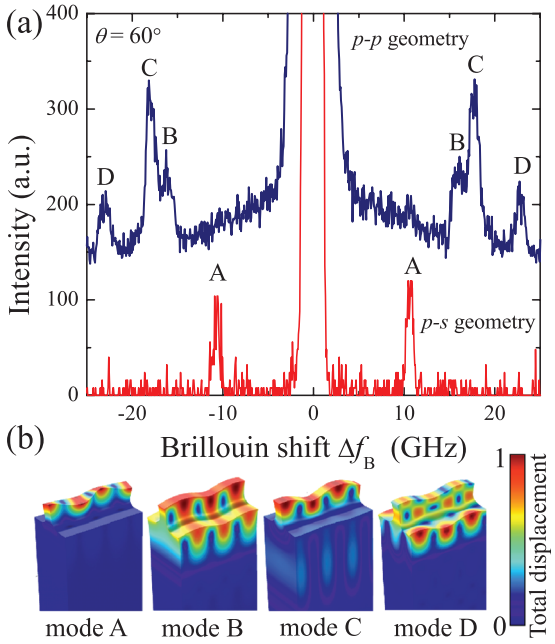

FIG. 2. (a) BLS spectra of a 1D surface phononic crystal for *p–p* and *p–s* geometry. (b) Corresponding FEM 3D deformation fields obtained for SAWs propagating in the [110] direction (parallel to the stripes) at $q = 0.020456$ nm^{-1}.

the mirror plane of a single stripe (without substrate) it is found that the displacement of mode A resembles an asymmetric (flexural) Lamb wave (LW) typically propagating in plates or membranes.[6,25,26] Figure 2(b) confirms also the experimentally found polarization of the B, C, and D modes. In particular, mode B, which is related to the deformation of the stripe as well as the substrate, is similar to a Rayleigh surface wave.[22,26] Mode C, the frequency of which is only slightly higher than that of mode B, propagates mainly in the stripe with small deformation of the substrate. On the other hand, mode D is related to a complex deformation of both stripe and substrate. Results of the angle resolved BLS obtained for several different angles θ are gathered in Fig. 3 as the dispersion relation $f_{SAW}(q)$. The experimental data are compared with the corresponding dispersion of SAWs calculated using FEM within the range of wavenumbers available in the BLS experiment. There is a good agreement between BLS data and the FEM calculations. From the FEM calculations shown in Fig. 3, it is seen that only mode B can propagate in the whole range of observed wavenumbers. It means that FEM solutions do not satisfy the criteria of Eq. (1) and waves related to A, C, and D modes exhibit bulk-like behavior for smaller wavenumbers.

The simplest SAW propagating near the free surface of homogeneous solid state medium known as RSW, are nondispersive (see Fig. 3). Generally, a RSW velocity depends on plane and direction of propagation and material properties such as elastic constants and mass density. Summing up the above results, it can be concluded that the significant disturbance of the free Si surface by the nanostructure in the form of periodic stripes leads to the presence of various dispersive SAWs propagating along the stripes/grooves. As shown in Fig. 3, all branches related to these SAWs lie below the line showing the dispersion of longitudinal bulk acoustic wave

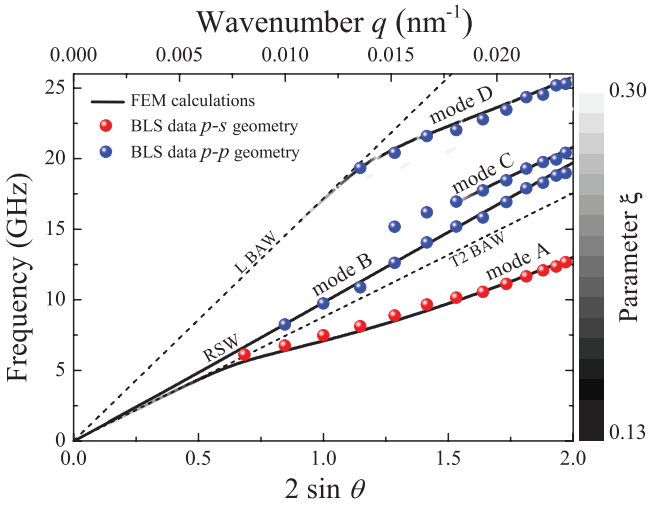

FIG. 3. Dispersion relation of SAWs propagating in [110] direction of a 1D surface phononic crystal. BLS experimental data (full circles) compared with FEM calculations (lines). Dashed lines show corresponding dispersion relations of longitudinal (L BAW), slower transverse (T2 BAW) bulk waves and Rayleigh surface wave (RSW) typical for Si.

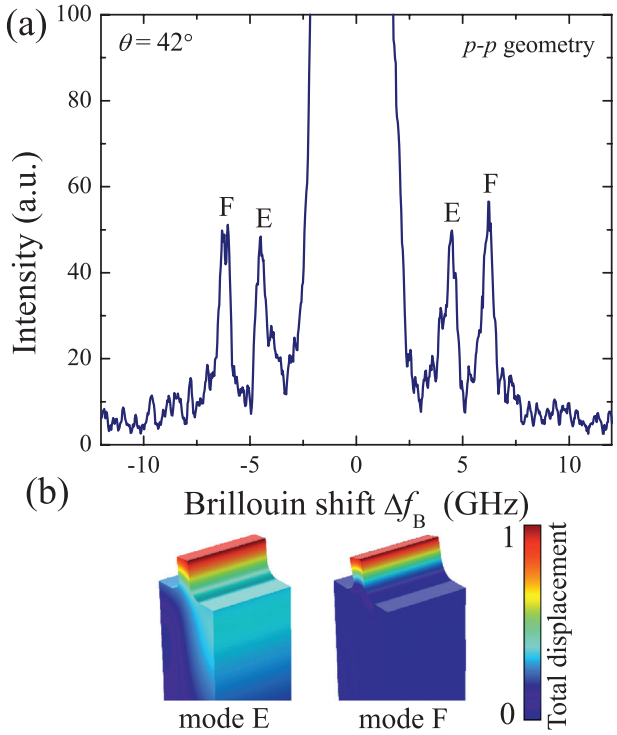

FIG. 4. (a) BLS spectra of a 1D surface phononic crystal for p–p geometry. (b) Corresponding FEM 3D deformation fields obtained for SAWs propagating in the $[1\bar{1}0]$ direction (normal to the stripes) at $q = 0.014542$ nm^{-1}.

(L BAW). In general, RSWs propagating along the [110] or $[1\bar{1}0]$ directions on the (001) plane of cubic crystals degenerate into slower transverse bulk waves (T2 BAW). Herein RSWs with phase velocity higher than that of the T2 BAW are observed simultaneously.[27] Considering mode A in Fig. 3, one can notice that for the wavelengths much longer than the sizes of the surface corrugation evolves gradually into T2 BAW. For shorter wavelengths, mode A is confined mainly in the stripe and its dispersion relation resembles that of quadratic-like asymmetric Lamb waves.[6,26] The dispersion of mode B is practically no different from that of the RSW of the flat Si substrate.

Experimental results obtained for SAWs propagating in the $[1\bar{1}0]$ direction (normal to the stripes) show a completely different behavior than SAWs described above. First of all, the particular BLS spectrum recorded with p–p geometry (see Fig. 4(a)) displays only two pairs of peaks. The corresponding displacement fields related to the SAWs are denoted here as modes E and F and are shown in Fig. 4(b). Here, they are completely polarized in the sagittal plane (x_1x_3). As mentioned above, our structure can be treated as a 1D SPnC, according to the Bloch theorem: $f_{SAW}(\mathbf{k}) = f_{SAW}(\mathbf{k} + \mathbf{G})$. Figure 5 compares the experimental (full circles) and calculated (lines) dispersion relations. Here, the range of wavenumbers available in the BLS experiment coincides with the first and second Brillouin Zone (BZ) of the SPnC. Similarly, as in Fig. 3, the dashed lines depict the dispersion of bulk and surface modes propagating in the particular direction of flat silicon. The branch denoted as mode F defines a frequency Bragg band gap opening at 7.83 GHz. The solutions of FEM calculations with higher frequencies are not visible here since they do not satisfy the criteria of SAW. This means that a well-designed periodic structure can partially or completely transform SAWs into BAWs, whereby mechanical energy is taken from the free surface into the bulk. Consequently, at frequencies higher than 7.83 GHz the considered structure can be treated as a good SAWs attenuator. As shown in Fig. 5, the presence of the low-frequency local resonance of the stripe splits the dispersion relation into two branches (mode E and F). Considering only the 1st BZ, mode E follows the RSW line for the small wavenumbers and continuously transforms through a low group velocity wave into the standing wave at the end of the 1st BZ. Here, mode E lies slightly below the local resonance frequency and the strain energy is mainly localized in the stripe (see Fig. 4(b)). Mode F propagates in a limited range of wavenumbers with a

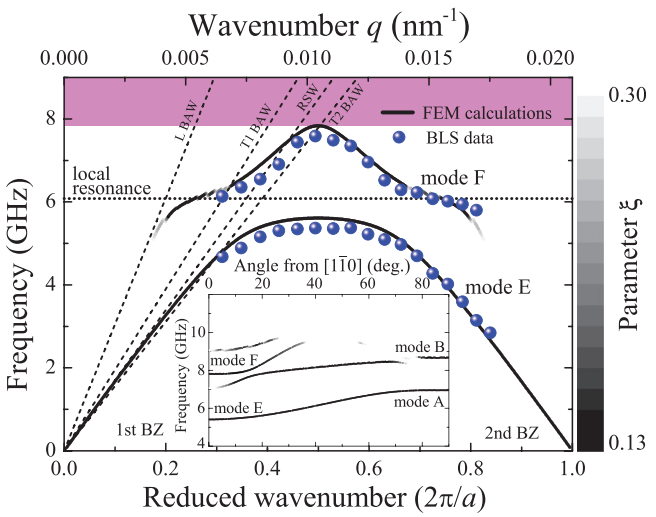

FIG. 5. Dispersion relation of SAWs propagating $[1\bar{1}0]$ direction of a 1D surface phononic crystal. BLS experimental data (full circles) compared with FEM calculations (lines). Dotted lines show the corresponding dispersion relations of longitudinal (L BAW), transverse (T1 BAW and T2 BAW) bulk waves, and Rayleigh (RSW) surface waves typical for Si. The inset presents the calculated angular dispersion of SAWs at $q = 0.0105$ nm^{-1}.

corresponding discontinuous branch and a strong variation of the ξ parameter. Solutions of mode F lying between sound lines of L BAW and T1 BAW result from the mixing of the local resonance and L BAW and T1 BAW, while those lying below T1 BAW line gradually follow the RSW line. It is worth mentioning that most of the previous studies on SPnCs were based on the concept of the sound cone limitation. The sound cone designates the part of band diagram lying above the sound line, the slope of which equals the speed of the slowest bulk wave (here T2 BAW) propagating in the given direction.[28] However, in our case, the modes which lie in this forbidden region are clearly observable and they are rather limited by the L BAW than by the T2 BAW. Therefore, instead of using this concept, we applied the criteria of Eq. (1) limiting surface-like solutions in the FEM calculations.

Summarizing the thermally activated hypersonic SAW propagating parallel and normal to the grating grooves were investigated by means of high-resolution Brillouin light scattering (BLS) supported by FEM calculations. Here, depending on the direction of SAWs propagation, both phononic properties (zone folding, band gap and local resonance interaction with bulk and surface waves) and also spatial confinement were observed.

The authors acknowledge the financial support from the FP7 FET Energy Project MERGING (Grant No. 309150); the Spanish MICINN projects nanoTHERM (Grant No. CSD2010-0044) and TAPHOR (MAT2012-31392). N.K. acknowledges support from the Micro and Nano Systems Center of Excellence - IMEL/NCSR DEMOKRITOS.

[1]N. Gomopoulos, D. Maschke, C. Y. Koh, E. L. Thomas, W. Tremel, H.-J. Butt, and G. Fytas, Nano Lett. **10**, 980 (2010).
[2]B. Graczykowski, S. Mielcarek, A. Trzaskowska, J. Sarkar, P. Hakonen, and B. Mroz, Phys. Rev. B **86**, 085426 (2012).
[3]W. Cheng, N. Gomopoulos, G. Fytas, T. Gorishnyy, J. Walish, E. L. Thomas, A. Hiltner, and E. Baer, Nano Lett. **8**, 1423 (2008).
[4]S. Bramhavar, C. Prada, A. A. Maznev, A. G. Every, T. B. Norris, and T. W. Murray, Phys. Rev. B **83**, 014106 (2011).
[5]V. A. Fonoberov and A. A. Balandin, Nano Lett. **5**, 1920 (2005).
[6]J. Cuffe, E. Chvez, A. Shchepetov, P.-O. Chapuis, E. H. El Boudouti, F. Alzina, T. Kehoe, J. Gomis-Bresco, D. Dudek, Y. Pennec, B. Djafari-Rouhani, M. Prunnila, J. Ahopelto, and C. M. Sotomayor Torres, Nano Lett. **12**, 3569 (2012).
[7]L. F. C. Pereira and D. Donadio, Phys. Rev. B **87**, 125424 (2013).
[8]X. Li, K. Maute, M. L. Dunn, and R. Yang, Phys. Rev. B **81**, 245318 (2010).
[9]Z. Xu and M. J. Buehler, Nanotechnology **20**, 185701 (2009).
[10]A. Alofi and G. P. Srivastava, Phys. Rev. B **87**, 115421 (2013).
[11]T. Still, W. Cheng, M. Retsch, R. Sainidou, J. Wang, U. Jonas, N. Stefanou, and G. Fytas, Phys. Rev. Lett. **100**, 194301 (2008).
[12]A. Khelif, Y. Achaoui, and B. Aoubiza, J. Appl. Phys. **112**, 033511 (2012).
[13]A. Balandin and K. L. Wang, Phys. Rev. B **58**, 1544 (1998).
[14]I. Ponomareva, D. Srivastava, and M. Menon, Nano Lett. **7**, 1155 (2007).
[15]D. L. Nika, E. P. Pokatilov, A. S. Askerov, and A. A. Balandin, Phys. Rev. B **79**, 155413 (2009).
[16]E. V. Castro, H. Ochoa, M. I. Katsnelson, R. V. Gorbachev, D. C. Elias, K. S. Novoselov, A. K. Geim, and F. Guinea, Phys. Rev. Lett. **105**, 266601 (2010).
[17]L. Lindsay, D. A. Broido, and N. Mingo, Phys. Rev. B **82**, 115427 (2010).
[18]D. A. Simons, J. Acoust. Soc. Am. **63**, 1292 (1978).
[19]S. R. Seshadri, J. Acoust. Soc. Am. **65**, 687 (1979).
[20]J. R. Dutcher, S. Lee, B. Hillebrands, G. J. McLaughlin, B. G. Nickel, and G. I. Stegeman, Phys. Rev. Lett. **68**, 2464 (1992).
[21]S. Lee, L. Giovannini, J. R. Dutcher, F. Nizzoli, G. I. Stegeman, A. M. Marvin, Z. Wang, J. D. Ross, A. Amoddeo, and L. S. Caputi, Phys. Rev. B **49**, 2273 (1994).
[22]L. D. Landau and E. M. Lifshitz, *Theory of Elasticity* (Pergamon Press, New York, USA, 1959).
[23]A. M. Marvin, V. Bortolani, and F. Nizzoli, J. Phys. C: Solid State Phys. **13**, 299 (1980).
[24]J. Sandercock, "Light scattering in solids III," in *Topics in Applied Physics*, edited by M. Cardona and G. Gntherodt (Springer, Berlin, Heidelberg, 1982), Vol. 51, pp. 173–206.
[25]H. Lamb, Proc. R. Soc. London, Ser. A. **93**, 114 (1917).
[26]I. A. Viktorov, *Rayleigh and Lamb Waves: Physical Theory and Applications* (Plenum Press, New York, 1967).
[27]G. W. Farnell, "Properties of elastic surface waves," in *Physical Acoustics* (Academic Press, New York, 1970), Vol. 6, pp. 109–166.
[28]A. Khelif, Y. Achaoui, S. Benchabane, V. Laude, and B. Aoubiza, Phys. Rev. B **81**, 214303 (2010).